J. Mech. Phys. Solids, 1973, Vol. 21, pp. 191 to 204. Pergamon Press. Printed in Great Britain.

IMPERFECTION-SENSITIVITY IN THE PLASTIC RANGE

By J. W. HUTCHINSON

Division of Engineering and Applied Physics,
Harvard University, Cambridge, Massachusetts

(*Received 4th September* 1972)

SUMMARY

THE EFFECT of small imperfections on the buckling of continuous structures loaded into the plastic range is studied. A simple model study is presented and several additional examples are discussed. The rôle of the load at which elastic unloading first occurs is emphasized, and a general asymptotic analysis is given for the behavior prior to the onset of elastic unloading for a class of elastic–plastic solids subject to loads characterized by a single load parameter. Asymptotic imperfection-sensitivity formulae are obtained whose features are similar to analogous formulae for elastic structures.

1. INTRODUCTION

AN ELASTIC structure which experiences a loss in load-carrying capacity as buckling deflections grow is imperfection-sensitive in the sense that small imperfections may significantly diminish the maximum load it can support. KOITER (1945, 1963) related the behavior of a slightly-imperfect structure to the post-buckling behavior of the perfect structure. If P_c denotes the bifurcation load of a perfect structure with an initially unstable post-buckling behavior, then the maximum support load $P^{\max}$ is related to the imperfection amplitude ξ by an asymptotic expression of the form

$$P^{\max} = P_c - C\xi^r + \ldots, \tag{1.1}$$

where C depends on the type of imperfection and other characteristics of the structure. The power r is either 1/2 or 2/3 depending on the nature of the bifurcation; *it is this singular behavior which magnifies the effect of a small imperfection.* A perfect structure which attains its maximum load at a limit point, rather than at a bifurcation point, does not generally display the strong sensitivity to small imperfections implied by (1.1) and its maximum support varies only linearly with small imperfections.

The lowest possible bifurcation to occur in a structure compressed into the plastic range almost always takes place under increasing load. Consequently, the maximum support load of the perfect structure is not attained at the bifurcation point but at a limit point following the occurrence of finite (perhaps small) bifurcation deflections. It is this feature of plastic buckling which makes an analytical treatment of imperfection-sensitivity difficult. We will argue that the load at which elastic unloading (strain-rate reversal) first occurs plays a pivotal rôle in the buckling imperfection-sensitivity of many structures. Furthermore, this quantity can be calculated asymptotically as a function of the imperfection amplitude since, in most problems of

interest, elastic unloading first begins in the perfect structure at the bifurcation point. With $\hat{P}$ denoting the load associated with the onset of elastic unloading, it will be shown that for small imperfections

$$\hat{P} = P_c - C\bar{\xi}^r + \ldots, \tag{1.2}$$

where P_c is the lowest bifurcation load of the perfect structure and in the most simple cases $r = 1/2$. Similar relations will be suggested as approximations to the buckling loads of structures with sufficiently large destabilizing material and geometrical nonlinearities.

The initial post-bifurcation behavior of continuous elastic–plastic solids was studied in a previous paper by the present writer (HUTCHINSON, 1973; henceforth referred to as (I)). The present paper uses the notation of (I) and at several points builds on developments given there. In the first part of the present paper the simple model which was introduced in (I) will be used to bring out some of the essential features of imperfection-sensitivity of continuous elastic–plastic structures. Several additional examples are discussed which illustrate the significance of the load at which elastic unloading starts; and a general analysis of the effect of imperfections on this load is given in Section 3.

2. IMPERFECTION-SENSITIVITY OF A SIMPLE MODEL

The effect of an imperfection on the behavior of the simple rigid-rod model pictured in Fig. 1 is considered where the imperfection is taken to be an initial rotation from the vertical, $\bar{\theta}$. The model has two overall degrees of freedom: the downward vertical displacement u and the total rotation from the vertical, $\theta+\bar{\theta}$. Spring elements are continuously distributed from $x = -L$ to $x = L$. At any point the contraction of a spring is

$$\varepsilon = u + x\theta \tag{2.1}$$

and the compressive force per unit length is denoted by s. At any point,

$$\left.\begin{aligned} \dot{s} &= E_t\dot{\varepsilon} \quad \text{for plastic loading,} \\ \dot{s} &= E\dot{\varepsilon} \quad \text{for elastic unloading or within the elastic range,} \end{aligned}\right\} \tag{2.2}$$

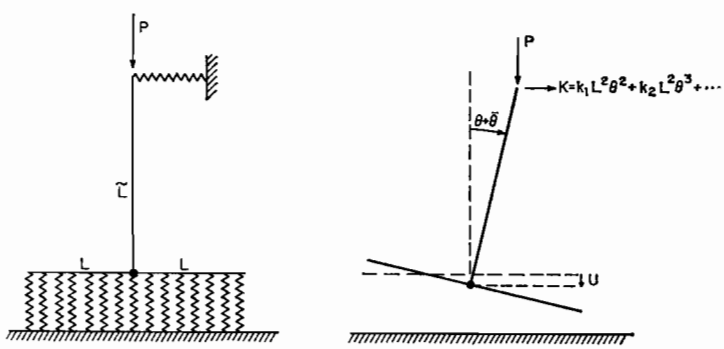

FIG. 1. A simple model for bifurcation and imperfection-sensitivity of continuous elastic–plastic solids in the plastic range.

where the tangent modulus E_t is considered to be a smooth function of s or ε. Nonlinear geometrical effects are incorporated into the model only through a nonlinear horizontal spring which develops a force $K = k_1 L^2\theta^2 + k_2 L^2\theta^3 + \ldots$ under rotation with the sign convention shown in Fig. 1. The equilibrium equations are

$$\dot{P} = \int_{-L}^{L} \dot{s}\, dx \tag{2.3}$$

and

$$[P\tilde{L}(\theta+\bar{\theta})]^{\cdot} + \dot{K}\tilde{L} = \int_{-L}^{L} \dot{s}\, x dx, \tag{2.4}$$

where P is the compressive load and $(\cdot)$ signifies a rate of change in the usual sense.

In the *elastic range* the relationship between P, θ and $\bar{\theta}$ for small θ is readily found to be

$$(P-P_c)\theta + k_1 L^2\theta^2 + k_2 L^2\theta^3 + \ldots = -P\bar{\theta}, \tag{2.5}$$

where $P_c = 2EL^3/(3\tilde{L})$ is the bifurcation load of the perfect model. If $k_1 \neq 0$ the asymptotic relation between the maximum support load $P^{\max}$ and $\bar{\theta}$ is

$$\frac{P^{\max}}{P_c} = 1-(6\kappa_1\bar{\theta})^{1/2} + \ldots \tag{2.6}$$

for $\kappa_1\bar{\theta} > 0$ where $\kappa_1 = \tilde{L}k_1/(EL)$. If $k_1 = 0$ and $k_2 > 0$ the asymptotic expression is

$$\frac{P^{\max}}{P_c} = 1 - \tfrac{3}{2}(3\kappa_2\bar{\theta}^2)^{1/3} + \ldots, \tag{2.7}$$

where $\kappa_2 = \tilde{L}k_2/(EL)$.

In the *plastic range* the lowest bifurcation load of the perfect model is given by $P_c = 2E_t^c L^3/(3\tilde{L})$ where E_t^c denotes the value of E_t at the bifurcation point. Post-bifurcation expansions about the lowest bifurcation load of the perfect model were given in (I). For the most interesting case in which $k_1 \geq 0$ and for $\dot{\theta} > 0$, the position d of the instantaneous elastic–plastic boundary starts from $x = -L$ and moves inward during the initial stages following bifurcation. The initial post-bifurcation expansions for $\bar{\theta} = 0$ and $\dot{\theta} > 0$ were found to be

$$\frac{P}{P_c} = 1 + a_1\theta + a_2\theta^{3/2} + a_3\theta^2 + a_4\theta^{5/2} + \ldots, \tag{2.8}$$

$$\frac{d}{L} = -1 - \tfrac{3}{2}b_2\theta^{1/2} - 2b_3\theta - \tfrac{5}{2}b_4\theta^{3/2} + \ldots, \tag{2.9}$$

where

$$a_1 = 3l, \qquad a_2 = 3lb_2 = -4l\left\{\frac{6lt_c - 2t_c' + 3\kappa_1}{3(1-t_c)}\right\}^{1/2}, \tag{2.10}$$

$$b_3 = \frac{3lt_c - t_c' - \kappa_1}{3(1-t_c)}, \qquad a_3 = 3lb_3 - 3l^2 - \frac{3l\kappa_1}{2t_c} + \frac{3lt_c'}{t_c}. \tag{2.11}$$

Here, it has been convenient to introduce the following non-dimensional quantities which appear above and in subsequent equations:

$$\left.\begin{aligned} l &= \frac{\tilde{L}}{L}, \qquad t = \frac{E_t}{E}, \qquad t_c = \frac{E_t^c}{E}, \qquad e = \frac{\varepsilon}{L}, \\ t_c' &= \left(\frac{dt}{de}\right)_c, \qquad t_c'' = \left(\frac{d^2t}{de^2}\right)_c, \qquad \kappa_1 = \frac{k_1\tilde{L}}{EL}, \qquad \kappa_2 = \frac{k_2\tilde{L}}{EL}. \end{aligned}\right\} \tag{2.12}$$

The slope of the load–rotation relation is initially positive but may be appreciably reduced after very small rotations. This would be expected, for example, if material and geometrical nonlinearities (as measured by $-t_c'$ and κ_1) are sufficiently large such that a_2 (which is negative) is large in magnitude compared to a_1. In this case the maximum support load $P_0^{\max}$ is only slightly larger than P_c. If just the first three terms on the right-hand side of (2.8) are used to estimate the maximum support load, one finds

$$\frac{P_0^{\max}}{P_c} = 1 + \tfrac{4}{27}\frac{a_1^3}{a_2^2}. \tag{2.13}$$

The analysis of the slightly-imperfect model separates into two problems. First, the behavior of the model is examined up to the first occurrence of elastic unloading where the values of applied load and rotation are denoted by $\hat{P}$ and $\hat{\theta}$. Secondly, perturbation expansions are developed about this state in a way which takes into account the expanding region of elastic unloading.

To analyze the behavior of the model prior to the occurrence of elastic unloading one can obviously suppress the unloading property of the stress–strain behavior and take the one-dimensional relation to be a nonlinear elastic one. Extending the meaning of HILL's (1961) terminology, we will refer to the model with the nonlinear elastic stress–strain relation as the *comparison model.* To obtain the behavior prior to elastic unloading at load levels approaching P_c, we analyze the comparison model using an initial post-buckling analysis of the Koiter-type. The result of this analysis gives the exact asymptotic equation:

$$\left(1 - \frac{P}{P_c}\right)\theta + a_1^e\theta^2 + \ldots = \rho\bar{\theta}, \tag{2.14}$$

where

$$\rho = \left(1 - \frac{t_c'}{3lt_c}\right)^{-1}, \qquad a_1^e = -\frac{3\rho\kappa_1}{2t_c} \tag{2.15}$$

and $P_c = 2E_t^c L^3/(3\tilde{L})$. Only the lowest order contribution of the imperfection, $\bar{\theta}$, has been retained. From (2.14) it is seen that a_1^e is the initial slope of the load–rotation relation of the perfect comparison model.

For $\bar{\theta} > 0$ with monotonically increasing P, elastic unloading will first occur at $x = -L$ when $\dot{\varepsilon} = \dot{u} - L\dot{\theta} = 0$. Thus, from (2.3) the slope of the load–rotation curve at the onset of elastic unloading is

$$\frac{\hat{\dot{P}}}{\dot{\theta}} = \int_{-L}^{L} \hat{E}_t(x)[L+x]\,dx, \tag{2.16}$$

where $\hat{E}_t(x)$ is the current value of the tangent modulus. For the perfect model, $\hat{P} = P_c$, $\hat{\theta} = 0$ and $\hat{E}_t = E_t^c$. The initial post-buckling analysis provides the following expression for E_t in terms of P and θ:

$$E_t = E_t^c + E\left(\frac{dE_t}{ds}\right)_c\left[\frac{(P-P_c)}{2EL} + x\theta\right] + O(\theta^2, (P-P_c)^2, \bar{\theta}). \tag{2.17}$$

It then follows from (2.16) that

$$\frac{1}{P_c}\frac{\hat{\hat{dP}}}{d\theta} = a_1 + O(\hat{\theta}, (\hat{P}-P_c), \bar{\theta}) \tag{2.18}$$

where the terms linear in $\hat{\theta}$ and $(\hat{P}-P_c)$ can easily be evaluated but will not be needed. Note that a_1 is the initial slope of the perfect model given by (2.10). In words, elastic unloading begins in the imperfect model when the slope of the load–rotation curve diminishes to the value a_1 corresponding to the initial slope of the perfect model (to lowest order).

To evaluate $\hat{P}$ and $\hat{\theta}$ use (2.14) with the condition (2.18). The results are

$$\hat{\theta} = \left(\frac{\rho\bar{\theta}}{a_1 - a_1^e}\right)^{1/2} + O(\bar{\theta}) \tag{2.19}$$

and

$$\frac{\hat{P}}{P_c} = 1 - (a_1 - 2a_1^e)\left(\frac{\rho\bar{\theta}}{a_1 - a_1^e}\right)^{1/2} + O(\bar{\theta}). \tag{2.20}$$

Now we go on to consider continuing deformation under increasing θ. For small but nonzero values of $\bar{\theta}$ it is possible to develop an expansion of P and the position d of the instantaneous elastic–plastic boundary about the state $(\hat{P}, \hat{\theta})$ in terms of integral powers of $(\theta - \hat{\theta})$. However, coefficients of this expansion are unbounded as $\bar{\theta} \to 0$ and consequently do not reduce to (2.8) and (2.9) in the limit for the perfect model. A *uniformly valid expansion*, which includes both perfect and imperfect cases, can be obtained in terms of an expansion parameter ζ which is defined for $\theta \geq \hat{\theta}$ by

$$\theta - \hat{\theta} = \gamma(\bar{\theta})^{1/2}\zeta + \zeta^2, \tag{2.21}$$

where the constant γ is determined in the expansion process. We omit the algebraic details required to carry out this expansion since they are quite lengthy and, to a certain extent, similar to those detailed for the perfect model in (I). The result is (for $\zeta \geq 0$ and $\zeta > 0$)

$$\frac{P}{Pc} = \frac{\hat{P}}{P_c} + p_1\zeta + p_2\zeta^2 + p_3\zeta^3 + \ldots, \tag{2.22}$$

$$\frac{d}{L} = -1 + d_1\zeta + d_2\zeta^2 + \ldots, \tag{2.23}$$

where the coefficients are given by

$$\gamma = -\frac{3cb_2(3lt_c - t_c')}{2(6lt_c - 2t_c' + 3\kappa_1)}, \qquad c = \left(\frac{\rho}{a_1 - a_1^e}\right)^{1/2}, \tag{2.24}$$

$$
\left.\begin{aligned}
&p_1 = a_1\gamma(\bar\theta)^{1/2}+O(\bar\theta), \qquad p_2 = a_1+p_2^{(1)}(\bar\theta)^{1/2}+O(\bar\theta),\\
&p_3 = a_2+p_3^{(1)}(\bar\theta)^{1/2}+O(\bar\theta), \qquad d_1 = -\tfrac{3}{2}b_2+d_1^{(1)}(\bar\theta)^{1/2}+O(\bar\theta),\\
&p_2^{(1)} = 9lb_2\gamma/4+2ct_c'(a_1^e-l)/t_c,\\
&p_3^{(1)} = -2ld_1^{(1)}+2lb_3\gamma+4lt_c'\gamma/t_c+ct_c'b_2(2a_1^e-3l)/t_c-9l(1-t_c)b_2^2\gamma/(16t_c),\\
&3(1-t_c)b_2d_1^{(1)} = -\tfrac{8}{3}t_c(p_2^{(1)}+a_2\gamma+a_3c)-12\kappa_2c+3(1-t_c)\gamma(b_2b_3+\tfrac{3}{16}b_2^3)+\\
&\qquad +\tfrac{2}{3}t_c'(4b_3c+7b_2\gamma)+\frac{3}{2l}ct_c'b_2^2(3l-a_1^e)+\tfrac{8}{3}ct_c''\left(-\tfrac{1}{5}+\frac{2a_1^e}{3l}\right).
\end{aligned}\right\} \tag{2.24}
$$

For $\bar\theta \to 0$, $\hat P = P_c$ and $\zeta = (\theta)^{1/2}$, and (2.22) reduces to (2.8) as already mentioned.

Two numerical examples are presented in Figs. 2 and 3 to illustrate the effect of small imperfections and to indicate the accuracy of the asymptotic expansions presented above. To bring in the material nonlinearity in a realistic way, quantities such as t_c, t_c', t'' were calculated using a Ramberg–Osgood type stress–strain relation, viz.

$$
\frac{\varepsilon}{\varepsilon_1} = \frac{s}{s_1}+\alpha\left(\frac{s}{s_1}\right)^n, \tag{2.25}
$$

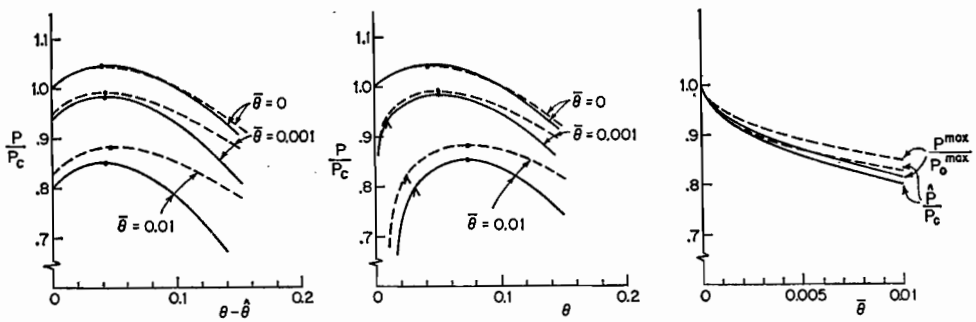

FIG. 2. Post-bifurcation behavior and imperfection-sensitivity of the model with material and geometrical nonlinearities ($\kappa_1 = 1$, $\kappa_2 = 0$). (Solid line curves are based on the asymptotic formulae; dashed line curves are obtained by numerical analysis.)

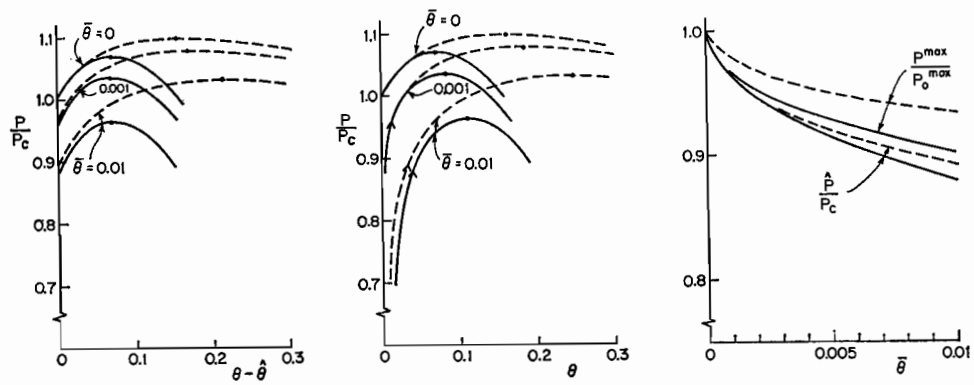

FIG. 3. Post-bifurcation behavior and imperfection-sensitivity of the model with only material nonlinearity ($\kappa_1 = \kappa_2 = 0$). (Solid line curves are based on the asymptotic formulae; dashed line curves are obtained by numerical analysis.)

where ε_1 and $s_1 = E\varepsilon_1$ are reference values. The solid line curves in these figures were obtained using the explicitly listed terms in (2.12), (2.14), (2.15) and (2.19) to (2.25). For both examples, $\alpha = 2/10$, $n = 3$, $l = 1$ and $(s_1/EL) = 0{\cdot}1094$ (corresponding to the values $E_t^c/E = 0{\cdot}46$ and $s_c/s_1 = 1{\cdot}4$, where s_c is the value of s at bifurcation). For comparison purposes a full numerical analysis was carried out for these two examples and these results are shown as dashed line curves in Figs. 2 and 3.†

In the first example, shown in Fig. 2, the model has a strong geometrical nonlinearity ($\kappa_1 = 1$, $\kappa_2 = 0$) in addition to the material nonlinearity associated with (2.25). In the elastic range the model has an asymmetrical bifurcation point with the imperfection-sensitivity implied by (2.6). On the left in Fig. 2 is shown the behavior following the onset of elastic unloading. Qualitatively, this family of curves can be viewed as being obtained by a downward translation of the curve for the perfect model such that the ordinate is intercepted at $\hat{P}$. Curves of P as a function of θ are shown in the center of Fig. 2. The point where elastic unloading starts is marked by a wedge and the point where the maximum load is attained is marked by a dot. On the right, plots of $\hat{P}/P_c$ and $P^{\max}/P_0^{\max}$ are given. The asymptotic results for $\hat{P}$ and $\hat{\theta}$ are reasonably accurate for imperfection amplitudes as large as those shown. Furthermore, the truncated series expansion (2.22) also gives a reasonably accurate estimate of the maximum support load for the perfect and slightly imperfect models.

For the example of Fig. 2 it is seen that

$$\frac{P^{\max}}{P_0^{\max}} \approx \frac{\hat{P}}{P_c} = 1-(a_1-2a_1^e)\left(\frac{\rho\bar{\theta}}{a_1-a_1^e}\right)^{1/2}+\ldots. \tag{2.26}$$

In fact, a calculation of $P^{\max}$ using the truncated series (2.22) shows that the approximation in (2.26) becomes increasingly accurate the larger is the parameter κ_1 measuring the geometrical nonlinearity. Certainly there is no general validity to (2.26) as will be seen; nevertheless, the curves of P/P_c vs. $(\theta-\hat{\theta})$ emphasize the pivotal rôle of the state $(\hat{P},\hat{\theta})$ marking the onset of elastic unloading. We have already remarked that elastic unloading starts in the imperfect model when the slope of the load–rotation curve diminishes to the value corresponding to the initial slope of the perfect model. In the presence of sufficiently large destabilizing geometric or material nonlinearities the slope diminishes rapidly with small further increase in load once elastic unloading starts.

No geometrical nonlinearity is present in the model for the example shown in Fig. 3 (i.e. $\kappa_1 = \kappa_2 = 0$). As a consequence the maximum load occurs at larger values $\theta-\hat{\theta}$ than in the first example. The truncated expansion (2.22) now loses accuracy prior to the occurrence of the actual maximum load point. Even in this example, however, the significance of $\hat{P}$ is evident, and the asymptotic formula for $\hat{P}/P_c$ gives a qualitative estimate of the effect of $\bar{\theta}$ on $P^{\max}/P_0^{\max}$.

The features illustrated by Figs. 2 and 3 are evident in the numerical results presented by DUBERG (1962) for a two-flanged column whose material properties are given by the Ramberg–Osgood relation (2.25). This column is analogous to the

† The numerical analysis of the model was carried out using a straightforward method. The range $-L \leq x \leq L$ was divided up into a large number of intervals in which the stress and strain was taken to be constant. Integrations in (2.3) and (2.4) were thereby replaced by summations over the intervals. Starting from zero applied load, the entire load–rotation curves shown were calculated incrementally using small changes in P (or θ). The curves for the perfect model were actually calculated using the numerical setup for the imperfect model with an extremely small imperfection ($\bar{\theta} = 10^{-6}$).

present model in the absence of any geometrical nonlinearity. His results indicate a sensitivity to small imperfections comparable to that in Fig. 3. A quantitative comparison of Duberg's numerical results for P^{max}/P_0^{max} with the predictions of a formula such as (2.26)† indicates somewhat better agreement than was found for the example of Fig. 3.

Further evidence of the approximate validity of (2.26) is provided by a discrete-element model analyzed by HUTCHINSON (1972). The analysis of that model directly yields the analog of (2.26) for cases in which the geometrical nonlinearity gives rise to strong imperfection-sensitivity in the elastic range. Somewhat similar behavior can be seen in the results of BATTERMAN (1971) for the effect of initial imperfections on a discrete arch model.

A final example which reveals the close proximity of $\hat{P}$ and P^{max} in both the perfect and imperfect structure is shown in Fig. 4. Shown there are load–deflection curves for the axisymmetrical deformation of a complete spherical shell subject to an external pressure p. These curves were obtained numerically and were taken from HUTCHINSON (1972), where a complete specification of the shell parameters is given. The material

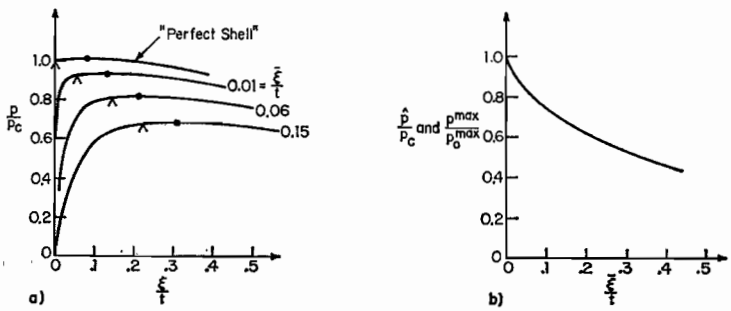

FIG. 4. (a) Curves of pressure as a function of buckling deflection for a complete spherical shell compressed into the plastic range. (b) Curves of maximum support pressure and pressure at the onset of elastic unloading as a function of imperfection amplitude.

comprising the shell is characterized by the J_2 flow theory of plasticity for a tensile stress–strain relation of the Ramberg–Osgood type (2.25) with $\alpha = 1/10$ and $n = 6$. The shell parameters are such that the stress at bifurcation is approximately 1·5 times the reference value s_1. The abscissa is the inward buckling deflection at the pole ξ normalized by the shell thickness t. The imperfection is in the form of the eigenmode of the perfect shell and its amplitude is denoted by $\bar{\xi}$. Numerical results for $\hat{P}/P_c$ and P^{max}/P_0^{max} as a function of $\bar{\xi}/t$ are shown as a single curve in Fig. 4 since they are essentially indistinguishable in this plot.

3. IMPERFECTION-SENSITIVITY OF THE ONSET OF ELASTIC UNLOADING IN AN ELASTIC–PLASTIC SOLID

Consider an elastic–plastic body subject to dead load surface traction per original area, λT_i^S, on S_T and prescribed displacements, λu_i^S, on S_u where the load parameter λ is taken to increase monotonically prior to the occurrence of any limit point. The

† The general formula (3.19) for $\hat{P}/P_c$ given later applies to the Duberg column.

reader is referred to (I, Sects. 3 and 4) for a specification of the notation and formulation which is used below. The undeformed configuration of the perfect body is used as the reference configuration. The imperfection is taken to be an initial stress-free distortion of the perfect configuration, $\xi\bar{u}_i$, where ξ is referred to as the amplitude of the imperfection. The total displacement from the reference configuration is $u_i+\xi\bar{u}_i$. Deformation from the initially imperfect state is measured by the difference between the Lagrangian strain tensor of the current state and that of the initial state, i.e.

$$\eta_{ij} = \tfrac{1}{2}(u_{i,j}+u_{j,i})+\tfrac{1}{2}u^k{}_{,i}u_{k,j}+\tfrac{1}{2}\xi(\bar{u}^k{}_{,i}u_{k,j}+\bar{u}^k{}_{,j}u_{k,i}). \tag{3.1}$$

Rates of change of the convected contravariant components of the Kirchhoff stress tensor are related to the strain-rate by

$$\dot{\tau}^{ij} = L^{ijkl}\dot{\eta}_{kl} \qquad \text{for} \qquad m^{kl}\dot{\eta}_{kl} \geq 0, \tag{3.2}$$

$$\dot{\tau}^{ij} = \mathscr{L}^{ijkl}\dot{\eta}_{kl} \qquad \text{for} \qquad m^{kl}\dot{\eta}_{kl} < 0 \tag{3.3}$$

when the yield condition is satisfied; when it is not, (3.3) holds.

The fundamental solution of the *perfect body* is denoted by u_i^0, η_{ij}^0, and τ^{0ij}. It is unique prior to the occurrence of the first possible bifurcation at $\lambda = \lambda_c$. We restrict consideration to problems in which there is no elastic unloading associated with the fundamental solution; furthermore, we will assume that the body becomes fully plastic prior to bifurcation. Many structures designed to be effective under compressive loadings fall within these restrictions—the axially compressed column is the most obvious example. Of primary interest are bifurcations occurring at loads below any limit point of the fundamental solution.

Assume that the eigenmode associated with λ_c is unique and denote it by $\overset{(1)}{u}_i$, $\overset{(1)}{\eta}_{ij}$ and $\overset{(1)}{\tau}{}^{ij}$. Normalize this mode in some definite way and denote its amplitude by ξ. Continuing with the convention adopted in (I) we will always take ξ to be positive and we will assume that ξ increases monotonically over the range of interest. To analyze the opposite-signed deflection in the eigenmode we will change the sign of $\overset{(1)}{u}_i$. HILL's (1958, 1961) bifurcation analysis requires that the bifurcation mode be a linear combination of an increment of the fundamental solution and the eigenmode

$$\dot{u}_i^0 + \overset{(1)}{u}_i = \lambda_1 u_i^{\prime 0} + \overset{(1)}{u}_i, \tag{3.4}$$

where

$$\dot{(\,)} = \frac{d(\,)}{d\xi} \qquad \text{and} \qquad (\,)' \equiv \left.\frac{d(\,)}{d\lambda}\right|_{\lambda_c}. \tag{3.5}$$

Here, λ_1 is the initial slope of the $\lambda-\xi$ relation for the perfect body (i.e. $\mathrm{d}\lambda/\mathrm{d}\xi|_{\lambda_c} = \lambda_1$). Furthermore, λ_1 must be sufficiently large such that plastic loading occurs throughout the body, that is

$$m_c^{ij}(\lambda_1 \eta_{ij}^{\prime 0} + \overset{(1)}{\eta}_{ij}) \geq 0. \tag{3.6}$$

In the absence of elastic unloading the branch (3.2) of the stress-rate–strain-rate relation can be regarded as the constitutive relation for a hypo-elastic solid as discussed in (I). However, before considering the behavior of the hypo-elastic comparison solid, we first discuss the analysis of the onset of strain-rate reversal in a nonlinear elastic solid (i.e. where L is derivable from a strain energy functional). The results for the

elastic solid are somewhat simpler than those for a general hypo-elastic solid and they provide a convenient lead-up to the more general analysis.

The initial post-buckling analysis of the elastic solid involves only a minor extension of the general KOITER (1945, 1963) analysis to include the effect of the variable moduli of the nonlinear stress–strain relation. We will not repeat this analysis here since it follows fairly closely a similar analysis given by FITCH (1968) and COHEN (1968) for the case of linear elastic solids. The asymptotic relationship between λ and ξ in the neighborhood of λ_c is found to be

$$(\lambda_c-\lambda)\xi+\lambda_1^e\xi^2+\ldots=\lambda\rho\bar{\xi}, \tag{3.7}$$

where only the lowest order effect of the imperfection, $\bar{\xi}\bar{u}_i$, is retained and λ_1^e and ρ are given by

$$\lambda_1^e=-\tfrac{1}{2}C^{-1}\int_V\left(3\overset{(1)}{\tau}{}^{ij}\overset{(1)}{u}{}^{k}{}_{,i}\overset{(1)}{u}{}_{k,j}+\overset{(1)}{\tau}{}^{mn}\frac{\partial L^{ijkl}}{\partial\tau^{mn}}\bigg|_c\overset{(1)}{\eta}_{ij}\overset{(1)}{\eta}_{kl}\right)dV \tag{3.8}$$

and

$$\rho=(\lambda_c C)^{-1}\int_V\{\tau_c^{0ij}\overset{(1)}{u}{}^{k}{}_{,i}\bar{u}_{k,j}+\overset{(1)}{\tau}{}^{ij}u_{k,i}^{0c}\bar{u}^{k}{}_{,j}\}\,dV, \tag{3.9}$$

where

$$C=\int_V\left(\overset{\cdot}{\tau}{}^{0ij}\overset{(1)}{u}{}^{k}{}_{,i}\overset{(1)}{u}{}_{k,j}+2\overset{(1)}{\tau}{}^{ij}\overset{\cdot}{u}{}^{0}_{k,i}\overset{(1)}{u}{}^{k}{}_{,j}+\overset{\cdot}{\tau}{}^{0mn}\frac{\partial L^{ijkl}}{\partial\tau^{mn}}\bigg|_c\overset{(1)}{\eta}_{ij}\overset{(1)}{\eta}_{kl}\right)dV. \tag{3.10}$$

The symbol λ_1^e is used to distinguish the initial slope of the elastic body from that of the hypo-elastic body, λ_1^{he}, to be introduced later. Note that when due to symmetry the $\lambda-\xi$ relation of the perfect elastic body is independent of the sign of ξ, then $\lambda_1^e=0$. For future reference we record the expansions of the displacements and stresses which are needed in the derivation of (3.7):

$$u_i=u_i^0(\lambda)+\xi\overset{(1)}{u}_i+\xi^2\overset{(2)}{u}_i+\ldots \tag{3.11}$$

and

$$\tau^{ij}=\tau^{0ij}(\lambda)+L_c^{ijkl}(\eta_{kl}-\eta_{kl}^0(\lambda))+\tfrac{1}{2}\xi^2\overset{(1)}{\tau}{}^{mn}\frac{\partial L^{ijkl}}{\partial\tau^{mn}}\bigg|_c\overset{(1)}{\eta}_{kl}+\xi(\lambda-\lambda_c)\overset{\cdot}{\tau}{}^{0mn}\frac{\partial L^{ijkl}}{\partial\tau^{mn}}\bigg|_c\overset{(1)}{\eta}_{kl}+$$
$$+O(\xi^3,\xi^2(\lambda-\lambda_c),\ldots). \tag{3.12}$$

As discussed in (I), we will investigate the behavior of the most interesting post-bifurcation branch and therefore we will take the sign of $\overset{(1)}{u}_i$ such that λ_1^e is either zero or negative. Then, λ_1 is the smallest value which satisfies (3.6) and for the perfect body elastic unloading starts at the bifurcation point. For the imperfect body "unloading" (i.e. strain-rate reversal) will start when for the first time at any point in the body

$$m^{ij}\dot{\eta}_{ij}=0. \tag{3.13}$$

To calculate $\dot{\eta}$ use the fact that $\eta=\eta^0(\lambda)+\xi\overset{(1)}{\eta}+O(\xi^2,\xi\bar{\xi})$ and expand terms which are dependent on λ in a Taylor series about λ_c; also write

$$m^{ij}=m_c^{ij}+(\tau^{mn}-\tau_c^{0mn})\frac{\partial m^{ij}}{\partial\tau^{mn}}\bigg|_c+\ldots. \tag{3.14}$$

One then finds

$$m^{ij}\dot{\eta}_{ij} = m_c^{ij}\left(\frac{d\lambda}{d\xi}\dot{\eta}_{ij}^{0} + \overset{(1)}{\dot{\eta}}_{ij}\right) + \mathrm{O}(\lambda-\lambda_c, \xi, \bar{\xi}). \tag{3.15}$$

Since λ_1 assumes the smallest value possible consistent with (3.6) we conclude that the value of $d\lambda/d\xi$ at which $m^{ij}\dot{\eta}_{ij}$ first vanishes is given by

$$\widehat{\frac{d\lambda}{d\xi}} = \lambda_1 + \mathrm{O}(\hat{\lambda}-\lambda_c, \hat{\xi}, \bar{\xi}) \tag{3.16}$$

exactly analogous to the behavior of the simple model. Condition (3.16) together with (3.7) provides the asymptotic expression for the values of λ and ξ associated with the onset of "unloading", namely,

$$\hat{\xi} = \left(\frac{\lambda_c \rho \bar{\xi}^2}{\lambda_1 - \lambda_1^e}\right)^{1/2}, \tag{3.17}$$

$$\frac{\hat{\lambda}}{\lambda_c} = 1 - \left(\frac{\lambda_1 - 2\lambda_1^e}{\lambda_c}\right)\left(\frac{\lambda_c \rho \bar{\xi}^2}{\lambda_1 - \lambda_1^e}\right)^{1/2}. \tag{3.18}$$

The formal similarity to the simple model expressions is evident. When $\lambda_1^e = 0$ (as it is, for example, for the compressed column discussed earlier) (3.18) reduces to the even simpler formula

$$\frac{\hat{\lambda}}{\lambda_c} = 1 - \left(\frac{\lambda_1 \rho \bar{\xi}^2}{\lambda_c}\right)^{1/2}. \tag{3.19}$$

Now we return to the analysis of the hypo-elastic comparison solid whose behavior does coincide with that of the elastic–plastic solid prior to the onset of elastic unloading. The comparison solid was introduced in (I, Sect. 5). The *stress* in a hypo-elastic solid depends on the deformation history. Here we will restrict attention to solids whose *moduli* exhibit no path dependence or can be taken to be approximately path independent in the region of strain space spanned by the solutions for the perfect and slightly-imperfect body. We assume that the moduli can be regarded as a function of the stress alone (as, for example, in the case of simple J_2 flow theory for small strain plasticity). As before, denote the fundamental solution of the perfect body by $\tau^0(\lambda)$, $\eta^0(\lambda)$, $\mathbf{L}_0(\lambda)$; and define $\Delta\mathbf{L} = \mathbf{L}-\mathbf{L}_0$ and $\Delta\eta = \eta-\eta^0$ for every value of λ. Then,

$$\dot{\tau}^{ij} - \dot{\tau}^{0ij} = L^{ijkl}\dot{\eta}_{kl} - L_0^{ijkl}\dot{\eta}_{kl}^0 = L_0^{ijkl}\Delta\dot{\eta}_{kl} + \Delta L^{ijkl}\dot{\eta}_{kl}, \tag{3.20}$$

where $(\dot{\cdot}) = d/d\xi$ and λ is regarded as a function of ξ. Thus,

$$\tau^{ij} - \tau^{0ij} = \int_0^{\xi} \{L_0^{ijkl}\Delta\dot{\eta}_{kl} + \Delta L^{ijkl}\dot{\eta}_{kl}\}\, d\xi. \tag{3.21}$$

Next, assume an expansion in the form of (3.11). Expand all quantities dependent on λ in a Taylor series about λ_c (e.g. $\mathbf{L}_0 = \mathbf{L}_c + (\lambda-\lambda_c)\dot{\tau}^0\, d\mathbf{L}/d\tau|_c + \ldots$) and then substitute in (3.21) with the result

$$\tau^{ij} = \tau^{0ij}(\lambda) + L_c^{ijkl}(\eta_{kl} - \eta_{kl}^0(\lambda)) + \tfrac{1}{2}\xi^2\, \overset{(1)}{\tau}{}^{mn}\frac{\partial L^{ijkl}}{\partial \tau^{mn}}\bigg|_c \overset{(1)}{\eta}_{kl} + \dot{\tau}^{0mn}\frac{\partial L^{ijkl}}{\partial \tau^{mn}}\bigg|_c \overset{(1)}{\eta}_{kl}\int_0^{\xi}(\lambda-\lambda_c)\, d\xi +$$

$$+ \overset{(1)}{\tau}{}^{mn}\frac{\partial L^{ijkl}}{\partial \tau^{mn}}\bigg|_c \dot{\eta}_{kl}^0\int_0^{\xi}\lambda\xi\, d\xi + \mathrm{O}(\xi^3, \xi^2(\lambda-\lambda_c), \ldots). \tag{3.22}$$

Since

$$\int_0^{\xi} (\lambda-\lambda_c)\, d\xi = (\lambda-\lambda_c)\xi - \int_0^{\xi} \dot{\lambda}\xi\, d\xi,$$

we note that (3.22) reduces to the expression (3.12) for the elastic solid except for an additional term

$$\left\{ \overset{(1)}{\tau}{}^{mn} \frac{\partial \dot{L}^{ijkl}}{\partial \tau^{mn}}\bigg|_c \dot{\eta}^0_{kl} - \dot{\tau}^{0mn} \frac{\partial \dot{L}^{ijkl}}{\partial \tau^{mn}}\bigg|_c \overset{(1)}{\eta}_{kl} \right\} \int_0^{\xi} \dot{\lambda}\xi\, d\xi. \tag{3.23}$$

It is readily shown that the term in the brackets vanishes identically if $\mathbf{L}$ is derivable from a strain energy potential.

From this point on the analysis follows that of the elastic solid very closely. The principle of virtual work in conjunction with the assumed expansions is used to generate the sequence of boundary-value problems for $\overset{(1)}{u_i}$, $\overset{(2)}{u_i}$, etc. in much the same way as has been discussed by BUDIANSKY and HUTCHINSON (1964), BUDIANSKY (1966), FITCH (1968) and COHEN (1968). The analysis provides the asymptotic equation relating λ and ξ in the neighbourhood of λ_c in the presence of small imperfections. This equation is found to be

$$(\lambda_c-\lambda)\xi + \lambda_1^e \xi^2 + \delta \int_0^{\xi} \dot{\lambda}\xi\, d\xi + \ldots = \lambda\rho\xi, \tag{3.24}$$

where λ_1^e and ρ are given by the previously listed expressions (3.8) and (3.9) and

$$\delta = C^{-1} \int_V \left\{ \dot{\tau}^{0mn} \frac{\partial \dot{L}^{ijkl}}{\partial \tau^{mn}}\bigg|_c \overset{(1)}{\eta}_{ij}\, \overset{(1)}{\eta}_{kl} - \overset{(1)}{\tau}{}^{mn} \frac{\partial \dot{L}^{ijkl}}{\partial \tau^{mn}}\bigg|_c \dot{\eta}^0_{ij}\, \overset{(1)}{\eta}_{kl} \right\} dV. \tag{3.25}$$

As already discussed, the integrand in the above integral vanishes identically for a non-linear elastic solid and thus $\delta = 0$ in this case. We have not fully explored the possible range of values of δ. However, for the special case of J_2 flow theory and compressive-type fundamental solutions which satisfy proportional loading, $\delta \leq 0$.

Denote the initial slope in the perfect ($\bar{\xi} = 0$) hypo-elastic comparison problem by λ_1^{he} (i.e. $\lambda = \lambda_c + \lambda_1^{he}\xi + \ldots$). From (3.24) one obtains

$$\lambda_1^{he} = [1-\tfrac{1}{2}\delta]^{-1}\lambda_1^e \tag{3.26}$$

and it is a simple matter to show that this agrees with the expression for λ_1^{he} derived in (I). The solution to (3.24) satisfying $\lambda = 0$ for $\xi = 0$ is (for $\delta < 1$)

$$\lambda = \lambda_c + [(1-\delta)\xi + \rho\bar{\xi}]^{-1/(1-\delta)} \times$$
$$\times \left\{ -\lambda_c(\rho\bar{\xi})^{1/(1-\delta)} + 2\lambda_1^e \int_0^{\xi} \zeta[(1-\delta)\zeta + \rho\bar{\xi}]^{\delta/(1-\delta)}\, d\zeta \right\}. \tag{3.27}$$

For values of λ near λ_c, (3.27) can be expanded in small values of $\bar{\xi}/\xi$ leading to the asymptotic equation

$$(\lambda_c-\lambda)\xi + \lambda_1^{he}\xi^2 + \ldots = \lambda_c \xi^{-\delta/(1-\delta)} \left(\frac{\rho\bar{\xi}}{1-\delta}\right)^{1/(1-\delta)}. \tag{3.28}$$

The condition for the onset of elastic unloading is still given by (3.16). Using (3.16) and (3.28) one finds the lowest order asymptotic expression for $\hat{\xi}$ and $\hat{\lambda}$ to be

$$\hat{\xi} = \frac{1}{1-\delta} \left(\frac{\lambda_c}{\lambda_1 - \lambda_1^{he}}\right)^{(1-\delta)/(2-\delta)} (\rho\bar{\xi})^{1/(2-\delta)} \tag{3.29}$$

and

$$\hat{\lambda} = \lambda_c - \left[\lambda_1 - \left(\frac{2-\delta}{1-\delta}\right)\lambda_1^{he}\right]\left(\frac{\lambda_c}{\lambda_1 - \lambda_1^{he}}\right)^{(1-\delta)/(2-\delta)} (\rho\xi)^{1/(2-\delta)}. \tag{3.30}$$

When $\delta = 0$, as it is for any nonlinear elastic solid or, for example, for any problem such as the column model where the stress is everywhere unidirectional, then (3.30) reduces to the expression (3.18) given previously. In general, however, the lowest order effect of an imperfection on the behavior of an elastic–plastic body prior to unloading involves a different power than KOITER (1945, 1963) found for elastic solids, equation (1.1).

4. DISCUSSION

Attention has been restricted to problems in which the fundamental solution of the perfect body has the property that continuing plastic deformation takes place throughout the body as the load is increased. The load marking the onset of elastic unloading is highly sensitive to small imperfections. Several examples have been cited which suggest that for sufficiently large material and/or geometrical nonlinearities the maximum support load occurs after relatively small deflections following the onset of unloading. Furthermore, the approximation suggested for the simple model, i.e.

$$\frac{P^{\max}}{P_0^{\max}} \approx \frac{\hat{P}}{P_c}, \tag{4.1}$$

may give at least a qualitative prediction of the effect of small geometrical imperfections on the buckling load.

One obvious limitation of the suggested approximation (4.1) is that in "elastic limit" in which bifurcation takes place within the elastic range the expressions for $\hat{P}/P_c$ do not reduce to the appropriate elastic results for $P^{\max}/P_c$. In a typical problem involving a structure subject to a compressive load, the bifurcation load may be, say, only ten to thirty per cent higher than the load at which plastic yielding starts. Then, certainly, the asymptotic formulas will not be accurate for load reductions larger than ten to thirty percent. A simple model study given earlier (HUTCHINSON, 1972) provides some further discussion of these limitations.

Finally, we note that the asymptotic formulas for the behavior prior to the onset of elastic unloading can easily be specialized to elastic–plastic systems with a finite number of degrees of freedom.

ACKNOWLEDGMENT

This work was supported in part by the National Aeronautics and Space Administration under Grant NGL 22-007-012, and by the Division of Engineering and Applied Physics, Harvard University.

REFERENCES

BATTERMAN, S. C. 1971 *Israel Jl. Technol.* **9**, 467.

BUDIANSKY, B. 1966 *Proc. Int. Conf. Dynamic Stability of Structures* (Edited by HERRMANN, G.), p. 83. Pergamon Press, Oxford.

BUDIANSKY, B. and HUTCHINSON, J. W. 1964 *Proc. 11th Int. Cong. of Appl. Mech.*, p. 636. Springer, Berlin.

COHEN, G. A. 1968 *AIAA J.* **6**, 1616.

1969 *Ibid.* **7**, 1407.

DUBERG, J. E. 1962 *Handbook of Engineering Mechanics* (Edited by FLÜGGE, W.), Ch. 52. McGraw-Hill, New York.

FITCH, J. R. 1968 *Int. J. Solids Structures* **4**, 421.

HILL, R. 1958 *J. Mech. Phys. Solids* **6**, 236.

1961 *Problems of Continuum Mechanics*, p. 155. SIAM, Philadelphia.

HUTCHINSON, J. W. 1972 *J. appl. Mech.* **39**, 155.

1973 *J. Mech. Phys. Solids* **21**, 163.

KOITER, W. T. 1945 Over de Stabiliteit van het Elastisch Evenwicht, Thesis, Delft. H. J. Paris, Amsterdam. (English translation: 1967. NASA TTF–10.)

1963 *Proc. Symposium on Nonlinear Problems* (Edited by LANGER, R. E.), p. 257. University of Wisconsin Press, Madison.